

A beam-theory based method to partition fracture modes in delaminated beams

Paolo S. Valvo¹

¹*Department of Civil Engineering (Structures), University of Pisa, Italy*
E-mail: p.valvo@ing.unipi.it

Keywords: Laminated beam theory, delamination, energy release rate, fracture modes.

SUMMARY. The paper presents a beam-theory based method to partition fracture modes in planar laminated beams affected by through-the-width delaminations. According to classical laminated beam theory, the axial, shear and bending deformabilities, as well as bending-extension coupling, are taken into account. The kinematics of crack growth is analysed by defining the crack-tip displacement rates as the relative displacements at the crack tip per unit crack extension. Besides, the crack-tip forces exchanged between the separating laminates are computed. Lastly, by considering the work done by the crack-tip forces for the corresponding crack-tip displacement rates, explicit expressions for the energy release rate and its modal contributions are deduced.

1 INTRODUCTION

Classical laminated plate theory [1] is commonly applied in the analysis of delamination fracture in composites [2, 3], since the delaminated laminates are modelled as assemblages of sublaminates connected by rigid or deformable joints and interfaces. Besides, delamination growth criteria usually assume that crack propagation occurs when the energy release rate, G , reaches a critical value, G_c [4]. In general, however, delamination cracks propagate under mixed-mode fracture conditions, so it becomes necessary to partition the energy release rate into two additive contributions, G_I and G_{II} , related to fracture modes I (opening) and II (sliding), respectively. To this end, various alternative, but not equivalent, methods have been proposed.

For rigidly connected sublaminates, Williams [5] developed a *global method* to partition the energy release rate, based on analysis of the global forces acting on the cracked laminate. Schapery and Davidson [6] observed that Williams' assumptions were not generally fulfilled for asymmetrically delaminated laminates and proposed a method based on classical plate theory. Alternatively, Suo and Hutchinson developed a *local method* [7], where the mode mixity, i.e. the ratio G_{II} / G_I , is determined by analysing the singular stress field at the crack tip of a semi-infinite crack between two infinite isotropic elastic layers. Recently, the local method has been extended to include the effects of shear forces at the crack tip [8] and orthotropic materials [9].

On the other hand, if the sublaminates are connected by a deformable interface, the modal contributions to G can be computed directly, based on the (peak) values of the interfacial stresses at the crack tip [10–13]. Nonetheless, Qiao and Wang [14], yet considering a deformable interface, proposed to evaluate the mode mixity via an adaptation of the local method. This approach appears somehow questionable since the local method, originally developed in the context of plane elasticity, assumes that a stress singularity is present at the crack tip, but this hypothesis does not hold true when the sublaminates are connected by a deformable (elastic) interface.

In this paper we show how the energy release rate associated with the growth of a delamination in a laminated beam can be partitioned into its modal contributions within the context of beam theory. To this aim, we consider a laminated beam, affected by a through-the-width delamination,

as an assemblage of three rigidly connected laminated beams. Each beam is modelled according to classical laminated beam theory, while taking into account the axial, shear and bending deformabilities, as well as bending-extension coupling. Under general load conditions, a small extension of the existing crack is considered. Thus, the kinematics of crack growth is analysed by defining the *crack-tip displacement rates* as the relative displacements occurring at the crack tip per unit crack extension. Besides, the *crack-tip forces* exchanged between the separating laminates are computed. Lastly, by considering the work done by the crack-tip forces for the corresponding crack-tip displacement rates, explicit expressions for the energy release rate and its modal contributions are deduced.

One example is presented to illustrate the effectiveness of the method.

2 DELAMINATED BEAM MODELLING

2.1 Beam-theory model of a delaminated laminate

Consider a laminate AB of length L , thickness $H = 2h$, and width B , affected by a through-the-width delamination of length a (Fig. 1). The delamination runs from the end section A to the intermediate section C, to which the crack tip C belongs, thus splitting the laminate into two sublaminates of thicknesses $H_1 = 2h_1$ and $H_2 = 2h_2$, respectively. We denote with $b = L - a$ the length of the unbroken part of the laminate, included between sections C and B.

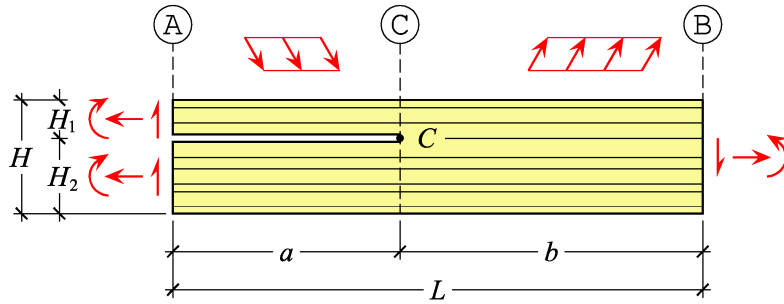


Figure 1: Delaminated laminate subjected to concentrated and distributed loads.

We suppose the laminate to be in equilibrium under the action of a known system of in-plane concentrated and distributed loads. Moreover, we assume that no out-of-plane effects are present, so that the delaminated laminate can be modelled as a planar laminated beam or, more precisely, as an assemblage of three planar laminated beams, each rigidly connected to the others at section C (Fig. 2a). In particular, beams 1 and 2 correspond to the upper and lower sublaminates, respectively, in the delaminated part of the laminate (between sections A and C), while beam 3 corresponds to the unbroken part (between sections C and B).

A rectangular reference system Ozx is fixed with the origin O at the intersection between the crack-tip cross section and the centreline of the unbroken part of the laminate, the x - and z -axes aligned with the laminate's axial and transverse directions, respectively (Fig. 2b). Correspondingly, we indicate with $u_\alpha(x)$ and $w_\alpha(x)$ the axial and transverse displacements of the beams' centrelines, and with $\phi_\alpha(x)$ their cross sections' rotations, positive if counter-clockwise (here and in the following the beams are identified by the subscripts $\alpha = 1, 2, 3$).

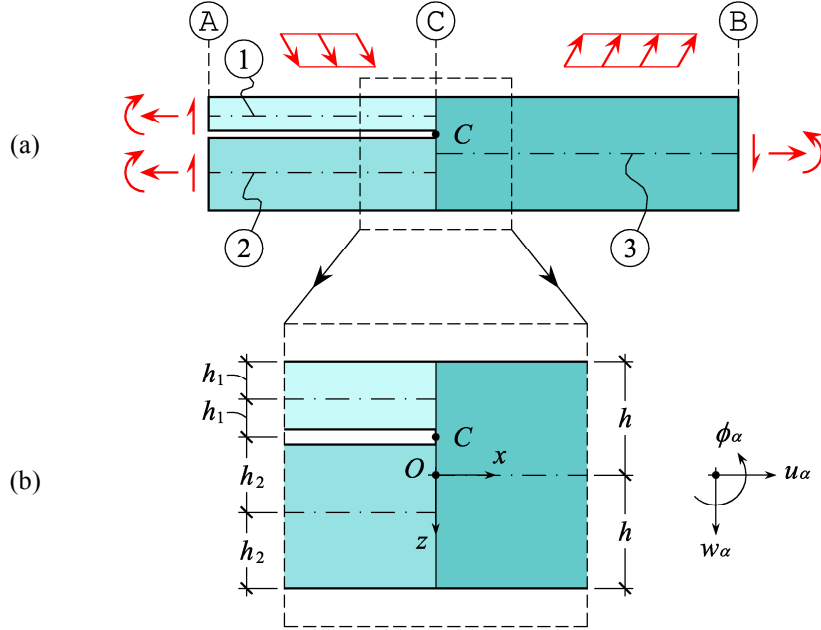


Figure 2: (a) The delaminated laminate as an assemblage of three laminated beams; (b) An enlargement of the crack-tip region and the fixed reference system.

According to Timoshenko's beam theory kinematics, we define

$$\varepsilon_\alpha(x) = \frac{du_\alpha}{dx}, \quad \gamma_\alpha(x) = \frac{dw_\alpha}{dx} + \phi_\alpha(x), \quad \kappa_\alpha(x) = \frac{d\phi_\alpha}{dx}, \quad (1)$$

respectively as the *axial strain*, *shear strain*, and *curvature*. The related internal forces in beams are the *axial force*, *shear force*, and *bending moment*, respectively, given by

$$N_\alpha(x) = B[A_\alpha \varepsilon_\alpha(x) + B_\alpha \kappa_\alpha(x)], \quad Q_\alpha(x) = B C_\alpha \gamma_\alpha(x), \quad M_\alpha(x) = B[B_\alpha \varepsilon_\alpha(x) + D_\alpha \kappa_\alpha(x)], \quad (2)$$

where A_α , B_α , C_α , and D_α respectively are the *extension stiffness*, *bending-extension coupling stiffness*, *shear stiffness*, and *bending stiffness* (per unit width) of the beams, computed according to classical laminated plate theory [1]. By inverting Eqs. (2), we obtain also

$$\varepsilon_\alpha(x) = [a_\alpha N_\alpha(x) + b_\alpha M_\alpha(x)]/B, \quad \gamma_\alpha(x) = c_\alpha Q_\alpha(x)/B, \quad \kappa_\alpha(x) = [d_\alpha N_\alpha(x) + M_\alpha(x)]/B, \quad (3)$$

where

$$a_\alpha = \frac{D_\alpha}{A_\alpha D_\alpha - B_\alpha^2}, \quad b_\alpha = -\frac{B_\alpha}{A_\alpha D_\alpha - B_\alpha^2}, \quad c_\alpha = \frac{1}{C_\alpha}, \quad d_\alpha = \frac{A_\alpha}{A_\alpha D_\alpha - B_\alpha^2}, \quad (4)$$

are the *extension compliance*, *bending-extension coupling compliance*, *shear compliance*, and *bending compliance* of the beams, respectively [1].

2.2 Crack-tip relative displacements and crack-tip displacement rates

Imagine now that a small segment S of the laminate is cut out in the neighbourhood of the crack tip C (Fig. 3a). Regardless of the actual load system applied to the laminate, if we exclude the presence of concentrated loads at the crack-tip cross section, the segment S will be in equilibrium under the internal forces acting on the cross sections close to the crack tip. Thus, for $x \rightarrow 0$, if we denote with N_1 , Q_1 , M_1 and N_2 , Q_2 , M_2 the internal forces in beams 1 and 2, respectively, the internal forces in beam 3 will be

$$N_3 = N_1 + N_2, \quad Q_3 = Q_1 + Q_2, \quad M_3 = M_1 + M_2 - N_1 h_2 + N_2 h_1. \quad (5)$$

Next, suppose that the crack propagates in a self-similar way, increasing its length by a small amount, Δa . Hence, the crack-tip segment S transforms into the segment S_0 (Fig. 3b), where the crack tip reaches a new position, identified by point D , and the point C splits into two points, C_1 and C_2 , belonging to beams 1 and 2, respectively. If crack growth occurs under fixed load conditions, the internal forces in the cross sections close to the crack tip do not change appreciably and S_0 can still be considered in equilibrium under the same internal forces acting on S .

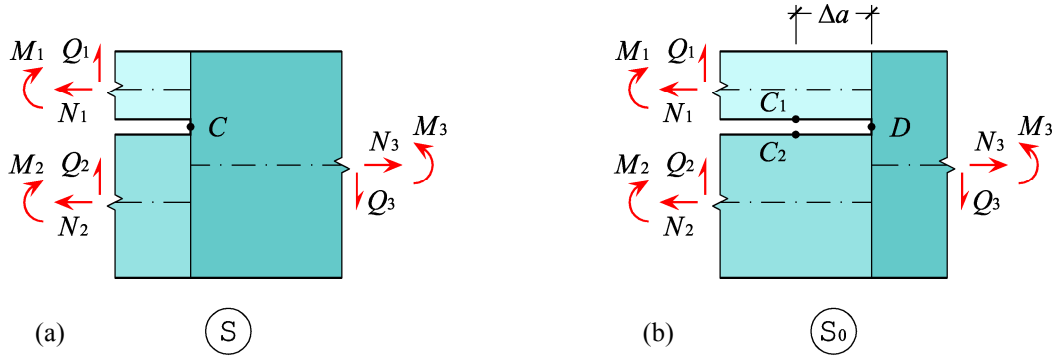


Figure 3: Elementary segments of the laminate in the neighbourhood of the crack tip: (a) S , before crack propagation; (b) S_0 , after crack propagation.

Obviously, however, the displacement compatibility is not preserved by going from S to S_0 , as in the latter system the points C_1 and C_2 generally undergo non-zero relative displacements (Fig. 4),

$$\begin{aligned} \Delta u &= u_{C_2} - u_{C_1} = (u_2 - \phi_2 h_2) - (u_1 + \phi_1 h_1), \\ \Delta w &= w_{C_2} - w_{C_1} = w_2 - w_1, \\ \Delta \phi &= \phi_{C_2} - \phi_{C_1} = \phi_2 - \phi_1, \end{aligned} \quad (6)$$

where all the (generalised) displacements are tacitly evaluated at the crack-tip section ($x = 0$).

2.3 Crack-tip forces

The displacement compatibility of system S can be recovered from S_0 by superimposing to the latter an auxiliary system, S_C , where suitable axial forces, N_C , transverse forces, Q_C , and couples, M_C , are exchanged between points C_1 and C_2 (Fig. 5).

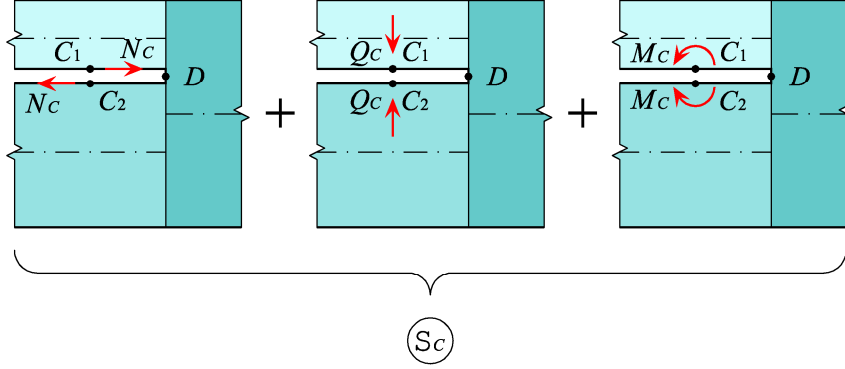


Figure 5: Crack-tip forces in system S_C .

The intensities of the above *crack-tip forces* are determined in such a way as to restore displacement compatibility previous to crack growth. To this aim, we compute the crack-tip displacement rates associated with system S_C , which turn out to be

$$\eta_u^C = -N_C \eta_u^N - M_C \eta_u^M, \quad \eta_w^C = -Q_C \eta_w^Q, \quad \eta_\phi^C = -N_C \eta_\phi^N - M_C \eta_\phi^M, \quad (10)$$

where

$$\begin{aligned} \eta_u^N &= \frac{1}{B} (\mathbf{a}_1 + \mathbf{a}_2 + 2\mathbf{b}_1 h_1 - 2\mathbf{b}_2 h_2 + \mathbf{d}_1 h_1^2 + \mathbf{d}_2 h_2^2), & \eta_u^M = \eta_\phi^N &= \frac{1}{B} (\mathbf{b}_1 + \mathbf{b}_2 + \mathbf{d}_1 h_1 - \mathbf{d}_2 h_2), \\ \eta_\phi^M &= \frac{1}{B} (\mathbf{d}_1 + \mathbf{d}_2), & \eta_w^Q &= \frac{1}{B} (\mathbf{c}_1 + \mathbf{c}_2), \end{aligned} \quad (11)$$

are generalised compliances, which describe the deformability of the crack-tip element.

Then, we require that

$$\eta_u + \eta_u^C = 0, \quad \eta_w + \eta_w^C = 0, \quad \eta_\phi + \eta_\phi^C = 0. \quad (12)$$

By substituting Eqs. (10) into (12) and solving for the crack-tip forces, we obtain

$$N_C = \frac{\eta_\phi^M \eta_u - \eta_u^M \eta_\phi}{\eta_u^N \eta_\phi^M - \eta_u^M \eta_\phi^N}, \quad Q_C = \frac{\eta_w}{\eta_w^Q}, \quad M_C = \frac{\eta_u^N \eta_\phi - \eta_\phi^N \eta_u}{\eta_u^N \eta_\phi^M - \eta_u^M \eta_\phi^N}. \quad (13)$$

3 ENERGY RELEASE RATE AND FRACTURE MODE PARTITIONING

3.1 Energy release rate

Under fixed load conditions [2], the energy release rate associated with crack growth is

$$G = -\frac{1}{B} \lim_{\Delta a \rightarrow 0} \frac{\Delta U}{\Delta a}, \quad (14)$$

where ΔU is the change in strain energy related to the increase in crack length Δa . According to the definitions given in the previous section,

$$\Delta U = U_0 - U, \quad (15)$$

where U and U_0 are the strain energies in systems S and S_0 , respectively. Since system S can be obtained by superimposing systems S_0 and S_C , it is also

$$U = U_0 + U_C, \quad (16)$$

where U_C is the strain energy in system S_C . By substituting Eq. (15) and (16) into (14), we obtain

$$G = \frac{1}{B} \lim_{\Delta a \rightarrow 0} \frac{U_C}{\Delta a}. \quad (17)$$

The strain energy stored in S_C can be evaluated by direct calculation, however it is more convenient to apply Clapeyron's theorem, which yields

$$U_C = \frac{1}{2}(N_C \Delta u + Q_C \Delta w + M_C \Delta \phi), \quad (18)$$

where Δu , Δw , and $\Delta \phi$ are the crack-tip relative displacements in system S_0 , given by Eqs. (7), which are equal in magnitude and opposite in sign to those caused by the crack-tip forces in S_C .

By substituting Eq. (18) into (17), and remembering Eqs. (8), we obtain the energy release rate as a function of the crack-tip forces and crack-tip displacement rates,

$$G = \frac{1}{2B}(N_C \eta_u + Q_C \eta_w + M_C \eta_\phi). \quad (19)$$

Furthermore, by substituting Eqs. (12) into (19), the energy release rate can be expressed in terms of the crack-tip forces only,

$$G = \frac{1}{2B}[\eta_u^N N_C^2 + (\eta_\phi^N + \eta_u^M) N_C M_C + \eta_\phi^M M_C^2 + \eta_w^O Q_C^2], \quad (20)$$

or, by substituting Eqs. (13) into (19), in terms of the crack-tip displacement rates only,

$$G = \frac{1}{2B} \left[\frac{\eta_\phi^M \eta_u^2 - (\eta_\phi^N + \eta_u^M) \eta_u \eta_\phi + \eta_u^N \eta_\phi^2}{\eta_u^N \eta_\phi^M - \eta_\phi^N \eta_u^M} + \frac{\eta_w^2}{\eta_w^Q} \right]. \quad (21)$$

3.2 Fracture mode partitioning

In planar fracture mechanics problems the energy release rate can be decomposed as

$$G = G_I + G_{II}, \quad (22)$$

where the addends G_I and G_{II} are related to the so-called opening and sliding fracture modes, respectively. In particular, the *opening mode*, or *mode I*, corresponds to a fracture process where the separating parts of material move away one from another perpendicularly to the direction of crack propagation; while the *sliding mode*, or *mode II*, occurs when the separating parts undergo a relative displacement parallel to the direction of crack propagation.

In our model, mode I is related to the crack-tip displacement rates η_w and η_ϕ , while mode II is related to η_u . However, some caution is required in order to correctly recognise the contributions to G related to each fracture mode. If we closely examine both Eqs. (20) and (21), it is apparent that the terms depending on Q_C and η_w contribute to G_I only (incidentally, these terms are relevant only if we include shear deformability in the analysis); on the other hand, the terms depending on N_C , M_C and η_u , η_ϕ are strongly tied one another and, hence, contribute to both fracture modes.

The key to solve the enigma of fracture mode partitioning is to start from determining the contribution G_{II} , which must be in the following form:

$$G_{II} = \frac{1}{2B} N_C^{II} \eta_u, \quad (23)$$

where

$$N_C^{II} = \frac{\eta_u}{\eta_u^N} \quad (24)$$

is the crack-tip axial force that would be able to cancel the crack-tip sliding displacement rate, η_u , if no crack-tip couple, M_C , were present. Remembering Eqs. (11) and (12), we observe that N_C^{II} is in general distinct from N_C , since the latter also contributes to cancel η_ϕ , but they coincide if $\eta_u^M = \eta_\phi^N = 0$. This happens, for instance, when the delaminated sublaminates are uncoupled in bending-extension ($b_1 = b_2 = 0$) and such that $d_1 h_1 = d_2 h_2$.

By substituting Eq. (24) into (23) and (23) into (22), we finally obtain the explicit expressions of the modal contributions to the energy release rate in terms of the crack-tip displacement rates

$$G_I = \frac{1}{2B} \left[\frac{(\eta_\phi - \frac{\eta_\phi^N}{\eta_u^N} \eta_u)^2}{\eta_\phi^M - \frac{\eta_\phi^N}{\eta_u^N} \eta_u^M} + \frac{\eta_w^2}{\eta_w^Q} \right], \quad G_{II} = \frac{1}{2B} \frac{\eta_u^2}{\eta_u^N}. \quad (25)$$

Expressions of G_I and G_{II} as functions of the crack-tip forces are here omitted for brevity.

4 AN EXAMPLE OF APPLICATION: THE ADCB TEST

As a first example of application, we consider the asymmetric double cantilever beam (ADCB) test (Fig. 6), used to measure the mixed-mode fracture toughness of composite laminates [15]. According to the global method [5], the ADCB test should be a case of pure mode I, however this prediction is contradicted by all other methods of analysis, such as the local method, the virtual crack closure technique, the elastic-interface based models and so on, which correctly distinguish the mixed-mode character of this test (see Ref. [13] for a detailed discussion on this topic).

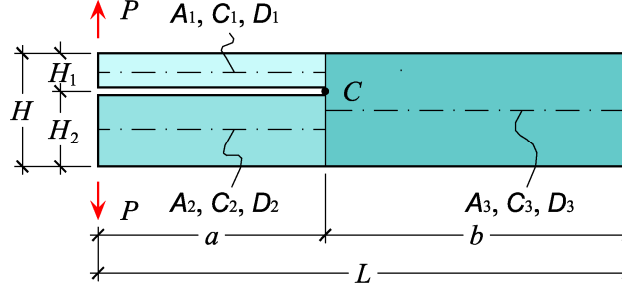


Figure 6: The asymmetric double cantilever beam (ADCB) test.

The internal forces at the crack-tip sections in this case are

$$N_1 = 0, \quad Q_1 = P, \quad M_1 = Pa; \quad N_2 = 0, \quad Q_2 = -P, \quad M_2 = -Pa. \quad (26)$$

By assuming that the delaminated laminates are uncoupled ($b_1 = b_2 = 0$), from Eqs. (8) we compute the crack-tip displacement rates,

$$\eta_u = \frac{Pa}{B}(d_1 h_1 - d_2 h_2), \quad \eta_w = \frac{P}{B}(c_1 + c_2), \quad \eta_\phi = \frac{Pa}{B}(d_1 + d_2), \quad (27)$$

and from Eqs. (11) we get the crack-tip compliances,

$$\begin{aligned} \eta_u^N &= \frac{1}{B}(a_1 + a_2 + d_1 h_1^2 + d_2 h_2^2), & \eta_u^M &= \eta_\phi^N = \frac{1}{B}(d_1 h_1 - d_2 h_2), & \eta_\phi^M &= \frac{1}{B}(d_1 + d_2), \\ \eta_w^Q &= \frac{1}{B}(c_1 + c_2). \end{aligned} \quad (28)$$

Hence, Eqs. (25) yield the mode I and II contributions to the energy release rate

$$G_I = \frac{P^2 a^2}{2B^2} [c_1 + c_2 + d_1 + d_2 - \frac{(d_1 h_1 - d_2 h_2)^2}{a_1 + a_2 + d_1 h_1^2 + d_2 h_2^2}], \quad G_{II} = \frac{P^2 a^2}{2B^2} \frac{(d_1 h_1 - d_2 h_2)^2}{a_1 + a_2 + d_1 h_1^2 + d_2 h_2^2}. \quad (29)$$

To confirm that the above result is correct, we notice that Eqs. (29) are identical with those that can be obtained from the elastic-interface model of the ADCB test [13] in the limit case of a rigid interface (i.e. when the elastic constants of the interface go to infinity).

5 CONCLUSIONS

We have presented a beam-theory based method to partition fracture modes in planar laminated beams affected by through-the-width delaminations. According to classical laminated beam theory, the axial, shear and bending deformabilities have been taken into account. Moreover, our analysis has included also *bending-extension coupling*, which, to our knowledge, has never been considered before by the fracture mode partitioning methods proposed in literature.

The kinematics of crack growth has been analysed by defining the *crack-tip displacement rates* as the relative displacements occurring at the crack tip per unit crack extension. These quantities appear as very helpful tools for fracture mechanics problems, since they sum up a description of the kinematics of crack growth. In this paper, we have used the crack-tip displacement rates to determine the explicit expressions of the crack-tip forces, energy release rate and modal contributions. Extension to planar and spatial elasticity problems looks promising.

Due to length restrictions, only one applicative example could be presented here. A more detailed explanation of the method and more examples will be presented in an extended paper.

References

- [1] Jones, R.M., *Mechanics of composite materials – 2nd ed.*, Taylor & Francis Inc., Philadelphia, PA (1999).
- [2] Friedrich, K. (editor), *Application of Fracture Mechanics to Composite Materials*, Elsevier, Amsterdam (1989).
- [3] Tay, T.E., “Characterization and analysis of delamination fracture in composites: An overview of developments from 1990 to 2001”, *Appl. Mech. Rev.*, **56**, 1–31 (2003).
- [4] Hutchinson, J.W., and Suo, Z., “Mixed mode cracking in layered materials”, *Adv. Appl. Mech.*, **29**, 63–191 (1992).
- [5] Williams, J.G., “On the calculation of energy release rates for cracked laminates”, *Int. J. Fract.*, **36**, 101–119 (1988).
- [6] Schapery, R.A. and Davidson, B.D., “Prediction of energy release rate for mixed-mode delamination using classical plate theory”, *Appl. Mech. Rev.*, **4**, S281–S287 (1990).
- [7] Suo, Z. and Hutchinson, J.W., “Interface crack between two elastic layers”, *Int. J. Fract.*, **43**, 1–18 (1990).
- [8] Li, S., Wang, J. and Thouless, M.D., “The Effects of Shear on Delamination of Beam-Like Geometries”, *J. Mech. Phys. Solids*, **52**, 193–214 (2004).
- [9] Andrews, M.G. and Massabò, R., “The effects of shear and near tip deformations on energy release rate and mode mixity of edge-cracked orthotropic layers”, *Eng. Fract. Mech.*, **74**, 2700–2720 (2007).
- [10] Allix, O. and Ladeveze, P., “Interlaminar interface modelling for the prediction of delamination”, *Compos. Struct.*, **22**, 235–242 (1992).
- [11] Corigliano, A., “Formulation, identification and use of interface models in the numerical analysis of composite delamination”, *Int. J. Solids Struct.*, **30**, 2779–2811 (1993).
- [12] Bruno, D. and Greco, F., “Mixed mode delamination in plates: a refined approach”, *Int. J. Solids Struct.*, **38**, 9149–9177 (2001).
- [13] Bennati, S., Colleluori, M., Corigliano, D. and Valvo, P.S., “An enhanced beam-theory model of the asymmetric double cantilever beam (ADCB) test for composite laminates”, *Comp. Sci. Tech.*, **69**, 1735–1745 (2009).
- [14] Qiao, P. and Wang, J., “Mechanics and fracture of crack tip deformable bi-material interface”, *Int. J. Solids Struct.*, **41**, 7423–7444 (2004).
- [15] Mangalgiri, P.D. *et al.*, “Effect of adherend thickness and mixed mode loading on debond growth in adhesively bonded composite joints”, NASA-TM-88992 (1986).